A Study of Alternative Lead Free Wave Alloys: From Process Yield to Reliability

Craig Hamilton[1], Mario Moreno[2], Ramon Mendez[2], German Soto[2], Jessica Herrera[2],
Teng Hoon Ng[3], Juthathip Fangkangwanwong[3]
Celestica Corporate (Toronto)[1], Celestica Mexico[2], Celestica Thailand[3]

Matthew Kelly[4], Jim Bielick[5]
IBM Corporation Toronto[4], IBM Corporation Rochester, MN[5]

Abstract
Recent industry trends have focused around alternatives for the commonly used SAC305 or SAC405 alloys for wave soldering and solder fountain rework processes. Industry consortia are currently focusing efforts on researching other "alternative Pb-free alloys" which are available on the market today [1]. Financial and technical reasons are driving many process engineers to consider an alloy change. The financial motivation is based on the increasing costs of the high silver content SAC alloys. With the constant pressure of having to reduce manufacturing costs, an opportunity to switch to a lower cost alloy for wave soldering would be a welcomed change. The cost of some of the alternative Pb-free alloys can be as little as half that of SAC – an attractive option. The technical reason for moving away from using SAC alloys for wave soldering and solder fountain processes may be even more significant. The high copper (Cu) dissolution rates which result from using SAC305/405 alloys for solder fountain rework have been documented as a major concern for the electronics industry [2,3]. The SAC305/405 Cu dissolution rates are so high that there is barely enough time to perform a 1X rework and in most cases do not allow enough contact time to perform a 2X solder fountain rework without experiencing irreparable damage to the PCB. This process limitation is a concern, especially for high reliability, long life products which may require multiple reworks during their lifetime. This technical issue in turn creates further financial impact through increased product scrap. To help address this technical issue, the evaluation of alternative Pb-free alloys continues. Previous work on some of these alternative Pb-free alloys has shown the benefits of having Cu dissolution rates similar to that of the 63Sn-37Pb alloy [4].

The financial and technical reasons for making a change away from using SAC305 or SAC405 alloys at wave solder and solder fountain are indeed compelling. However, before making a change to an alternative Pb-free alloy, a number of questions need to be answered, such as, what alternative Pb-free alloy/s should be considered? Which alternative Pb-free alloy/s offers the best process yield? Which offer the best thermal and mechanical reliability? As these alternative Pb-free alloys are relatively new to the electronics industry and therefore data limited, further study of their reliability performance is essential. A number of comprehensive investigations studying the reliability of PTH structures assembled with SAC and select alternative Pb-free wave alloys have been published to date [1,5-8].

This paper, an evolution of earlier work on this topic, discusses results obtained from an internally designed PTH test vehicle constructed to evaluate three commercially available alternative Pb-free wave alloys (Sn-Cu-Ni, Sn-Ag-Cu-Bi and Sn-Cu-X) by comparing their performance to SAC405 and SnPb. The process performance of each alloy is discussed, including profile optimization and process yield analysis. Failure analyses are presented to identify and explain observed failure mechanisms. In addition, the thermal and mechanical reliability analysis of each alloy is discussed. The objective of this work is to select a suitable wave alloy replacement to SAC305/405 that provides similar if not better overall solder joint quality as well as thermal and mechanical reliability.

Introduction
The benefits of some of the currently available alternative Pb-free alloys make them suitable replacements for the highly corrosive SAC alloys at the PTH rework process. An ideal manufacturing environment however would use a common solder alloy for both the solder fountain and wave process in order to maintain consistency and eliminate potential alloy mixing between the two processes. That being said, before implementing any alternative Pb-free alloy within either process, it is required to establish that they are comparable, if not superior, to SAC305 or 405 in both quality and reliability. Due to their lower silver content, most of these alternative Pb-free alloys are less expensive than SAC. However, if these alloys contribute to a decrease in yield after the wave soldering process, the additional rework required, depending on the extent of defects, would offset any upfront savings in alloy cost. In addition to confirming the process performance of these alternative Pb-free alloys, it is necessary to validate both the thermal and mechanical reliability of the alloy. Through-hole solder joints are historically known to be very reliable. The greater concern is the reliability of solder joint connections formed during the glue and wave SMT process. Both types of solder joints however need to be addressed.

The specific alloys included in this study, along with their respective melting ranges are listed in Table 1. This short list of alternative Pb-free alloys is comprised of those alloys from earlier work which exhibited reduced Cu dissolution rates compared to SAC305 and 405 alloys [4]. The three alternative Pb-free alloys selected are compared to both SnPb and SAC405.

Table 1. List of Alloys Studied

ALLOYS		MELTING RANGE
63Sn-37Pb	(SnPb)	183°C
95.5Sn-3.8Ag-0.7Cu	(SAC405)	217°C to 220°C
99.1Sn-0.7Cu-0.05Ni-(<0.01)Ge[1]	(Sn-Cu-Ni)	227°C
99.1Sn-0.7Cu-X-Y	(Sn-Cu-X)	227°C
98.6Sn-0.3Ag-0.7Cu-Bi-X-Y[2]	(Sn-Ag-Cu-Bi)	217°C to 228°C
1. U.S. Patent # 6180055	2. Patent # PCT/GB2005/004609	

The experimental phases of this study are listed in Table 2 below. While previous work focused solely on the compatibility of these alloys with the PTH rework process, this work focuses on the primary wave solder attach process. All alloys were subjected to wave profile optimization and verification Phases (1 and 2) in order to establish the optimized wave profile for each alloy. Due to test chamber capacity limitations, only SAC405 and the top two performing alternative Pb-free alloys, chosen based on Phase 2 results and other contributing factors, were included in the ATC (0-100°C) thermal reliability phase (Phases 3 and 4). Within Phases 3 and 4, a series of test vehicles were assembled and reworked with each of the alloys selected, and alloy yields were calculated based on the established optimized profiles. In addition, a series of boards was subjected to 1X and 2X PTH rework operations, along with hand repair, using the same alloy as primary attach. Finally, as few ATC failures were anticipated, in order to clearly rank the alternative Pb-free alloys, Phases 5 and 6 were included to study the mechanical and mechanical + thermal reliability of all five alloys included in the study.

This paper will include the results of Phases 1, 2, 3 (primary attach yield only), 5 and 6 (partial thermal/mechanical results). The rework performance and thermal reliability, ATC test (0-100°C, 6,000 cycles) results will be published in a future paper.

Table 2. Experimental Build Matrix

Phase	Description	Alloy	Profile Used	ATC	HTS	Sample Size
1	Wave Profile Optimization DoE	SnPb	DoE	N/A	N/A	8
		SAC405				36
		Alloy A				36
		Alloy B				36
		Alloy C				36
2	Wave Profile Verification Trials	SnPb	Optimized	N/A	N/A	10
		SAC405				10
		Alloy A				10
		Alloy B				10
		Alloy C				10
3	Primary Attach for ATC/yield/DFM	SAC405	Optimized	0 - 100°C 6,000 cycles	N/A	16
		1st Place Yield Performer from Phase 2				16
		2nd Place Yield Performer from Phase 2				16
4	1X & 2X PTH rework, 1X hand repair & Cu dissolution DoE	SAC405	Optimized			10
		1st Place Yield Performer from Phase 2				10
		2nd Place Yield Performer from Phase 2				10
5	Mechanical Testing (4 pt. bend & lead pull)	SnPb	Optimized	N/A	N/A	5
		SAC405				5
		Alloy A				5
		Alloy B				5
		Alloy C				5
6	Mechanical + Thermal Testing (static & dynamic load)	SnPb	Optimized	0 - 100°C (cycled to failure)	125°C (cycled to failure)	4
		SAC405				4
		Alloy A				4
		Alloy B				4
		Alloy C				4

Test Vehicle and Components

In order to study these alternative Pb-free wave alloys, a test vehicle (Figure 1a and 1b) was designed which incorporated a variety of PTH and bottom side SMT glue and wave components (see Table 3). The test vehicle incorporates daisy chain circuitry to measure any changes in electrical resistance during thermal and mechanical reliability testing. All SMT components, as well as nine PDIP components per board, are daisy chained for in-situ resistance monitoring. The test vehicle was designed to represent a mid-level complexity printed circuit board (PCB). The dimensions are 203mm x 254mm (8.0" x 10.0"), with a thickness of 2.36mm (0.093"). It consists of a total of 12 layers, with 4 (2 ounce) ground layers. It has an OSP surface finish (to represent the most difficult soldering conditions) and a high Tg FR-4 laminate, suitable for Pb-free wave soldering processing. The test vehicle also incorporates certain DFM design features such as: pin-to-hole ratio, component pitch, land pattern variation, orientation and ground plane/style connections. The impacts of these features are not discussed in this paper.

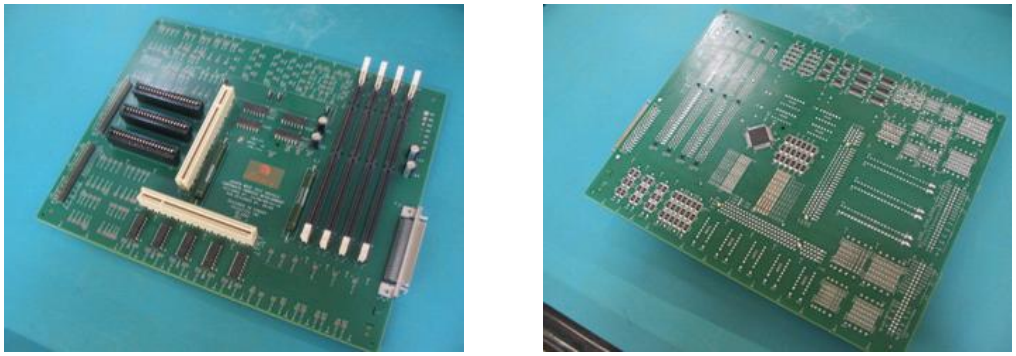

(a) **(b)**

Figure 1. (a) "Jasper" Test Vehicle (topside) ; (b) "Jasper" Test Vehicle (bottomside)

Table 3. List of Components Assembled

Components	Component Type	Qty / Board
Amplimite, 68 pin, 50mil pitch	PTH	1
Power Connector, 40 pin, 100mil pitch	PTH	3
PCI Slot Connector, 120 pin, 50mil pitch	PTH	2
DIMM Connector, 168 pin, 50mil pitch	PTH	4
PDIP Connector, 14 pin, 100mil pitch	PTH	9
Header, 40 pin, 100mil pitch	PTH	2
Electrolytic Capacitor, 2 pin, 140mil pitch	PTH	4
U-Anchor Connector, 2 pin, 200mil pitch	PTH	4
Ceramic Axial Resistor, 2 pin	PTH	2
SOIC8	SMT	6
SOIC16	SMT	6
SOT23	SMT	20
Resistor 0603	SMT	180
Resistor 0805	SMT	180
Resistor 1206	SMT	36
Resistor 2512	SMT	54
Capacitor 0603	SMT	45
Capacitor 0805	SMT	45
QFP64, 35mil pitch	SMT	1

Experimental and Testing Methodology

The experimental and testing methodology followed in each phase is described below.

Wave Profile Optimization, Assembly and Inspection

In order to optimize the SnPb wave profile, a 2x2 full factorial design of experiment (DoE) was defined and executed (Table 4). To optimize the Pb-free alloys, a Taguchi L36 (3x2x2) DoE was performed (Table 5). All four Pb-free alloys used the same DoE factors and levels. The DoE levels selected for pot temperature fell within the supplier recommended upper and lower limits for each alloy. Since there is a wider range of recommended pot settings due to the differing melting temperatures of the alternative alloys tested, three levels were selected for this factor to cover the entire range. The preheat temperature and contact time levels were established based on the upper and lower recommendations of the flux chemistry used. All DoE and final optimized boards assembled were pre-conditioned to represent a double sided reflowed board, and worst case soldering conditions. The DoE and final optimized sample sizes built for each alloy are listed in Table 2.

Table 4. SnPb Design of Experiment

Factors	Levels	
Pot Temperature (°C)	Constant at 250°C	
Preheat Temperature (°C)	Low	High
Contact Time (sec)	Low	High

Table 5. Pb-free Design of Experiment

Factors	Levels		
Pot Temperature (°C)	Low	Medium	High
Preheat Temperature (°C)	Low	-	High
Contact Time (sec)	Low	-	High

To reduce the complexity of the DoE, and in order to truly compare each alloys relative performance, the majority of the wave parameters were maintained as constants throughout the profile optimization and assembly phase (Table 6).

Table 6. Experimental Constants

Wave Configuration	Drilled Chip Bar & Contour
Atmosphere	Air
Preheat Configuration	2 top heaters (IR/Conv) & 3 bottom heaters (IR/Conv/Conv)
Fluxer	Spray Flux
Flux Type	No Clean, Alcohol Based
Flux Amount	Volume within Supplier Recommendations
Fixture Design	Open Pallet

All boards were visually inspected to document all wave solder related defects (i.e. solder bridges, excessive solder, solder balling etc…) and x-rayed, using a 5DX laminography x-ray inspection system, to measure the barrel fill of each PTH barrel. All visual and barrel fill related defects were inspected based on Class 2, IPC-A-610D specifications[9].

Thermal and Mechanical Reliability

4-Point Bend Test

Five boards per alloy were wave soldered with a center array of 2512 daisy chained resistors (qty 18), which were glued to the bottom side of each test vehicle (Figure 2). No other component was assembled. The 4-point bend testing was performed according to IPC-JEDEC-9702 standards[10]. Even though discrete SMT devices such as 2512 resistors are outside the scope of this test method, the test was still performed in order to provide a relative comparison between each of the wave alloys tested via a glue and wave process. The set-up of the test is illustrated in Figure 3 below. Strain gauges and resistance monitoring wires were attached to each board during the 4-point bend test. The strain gauges measured the strain vs. time during testing and the resistance through the array of 2512 resistors was monitored. The test vehicle was deflected between 4 – 8mm in 1mm increments until a 20% increase in resistance occurred. This is the distance the load span moved after making contact with the board. Maximum card deflection at the centre of the card was not measured. The load starting point was a distance of 200mm between the load span and the card, to allow the load head to attain full speed prior to contact with card.

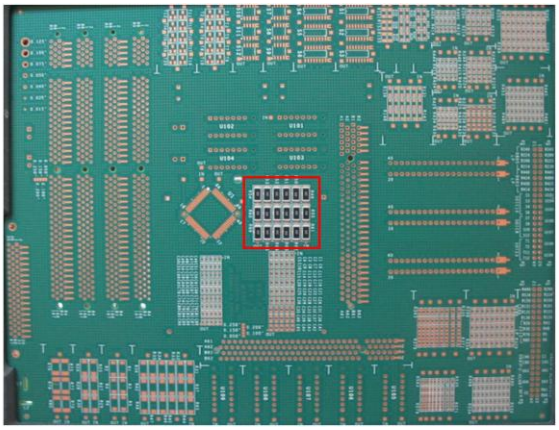

Figure 2. 4-point Bend 2512 Test Board

Figure 3. 4-point Bend Test Set-up

Lead Pull Test

A single 0.5mm QFP component was glued and wave soldered on each of the optimized test vehicles, using all 5 alloys (Figure 4). The test plan followed is illustrated in Table 7 below. All QFP bodies were carefully removed, and a total of 48 QFP leads per alloy (3 leads per side of each QFP) were pulled with a strain rate of 2.54mm/min and the maximum load to failure was measured. Additional leads were pulled if a lifted pad occurred, in order to obtain at least 32 solder-to-solder fails for statistical significance. The test set-up is illustrated in Figure 5 below.

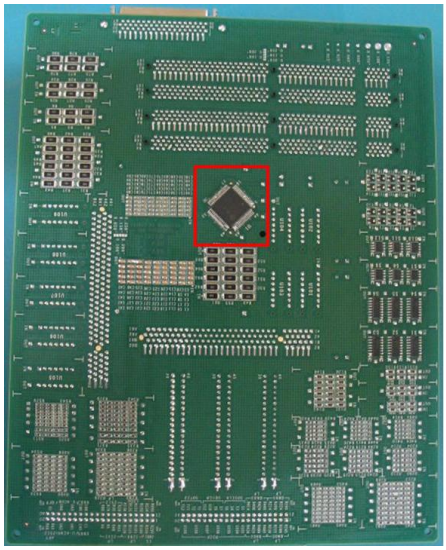

Figure 4. 0.5mm QFP

Table 7. Lead Pull Test Matrix

Board Qty	Alloy	# of Lead Pulls	Sample Size
1	SnPb	12	48
2		12	
3		12	
4		12	
1	SAC405	12	48
2		12	
3		12	
4		12	
1	Alloy A	12	48
2		12	
3		12	
4		12	
1	Alloy B	12	48
2		12	
3		12	
4		12	
1	Alloy C	12	48
2		12	
3		12	
4		12	

Figure 5. Lead Pull Test Set-up

Static and Dynamic Load Test

Two pairs of U-clips were assembled at locations UA1 through UA4, using each alloy type (4 boards per alloy). All of the U-clips after assembly were inspected for 100% barrel fill. This was a requirement for this phase of study, to insure that all alloys were tested under the same barrel fill conditions. The test plan followed is illustrated in Table 8. Each pair of U-clips was subjected to two levels of spring loads (16 and 32 lbs per clip) using a spring load device illustrated in Figure 6. A thermal ship shock was simulated on all boards, using -40°C to +65°C, over 5 cycles. On half the population of boards, an intentional 3% bow and twist was induced by using a mounting plate with a raised central mounting post (Figure 7). In addition, half of the population underwent mechanical shock and vibration. The mechanical shock profile used a 25g, 20ms Trapezoidal pulse, and 100g, 3ms Sine pulse, both 3-axis (two edges, and flat drop). The mechanical vibration parameters used consisted of a 1.0g RMS random, 15 minutes per board, between 2 to 200 Hz. The boards were then divided into either an accelerated thermal cycling (ATC) test or high temperature storage (HTS). Half of the boards (by alloy), were subjected to an ATC profile of 0-100°C, 1 cycle per hour on un-mounted boards (Figure 8) and the boards mounted to the 3% bow and twist fixtures were subjected to an HTS 125°C Isothermal bake (Figure 9).

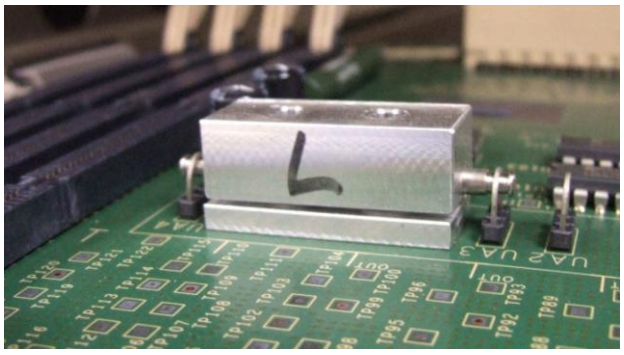

Figure 6. Spring Load Mechanism (U-clips)

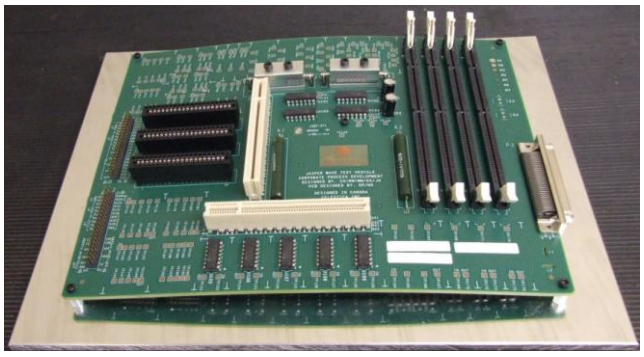

Figure 7. Bow and Twist Fixture

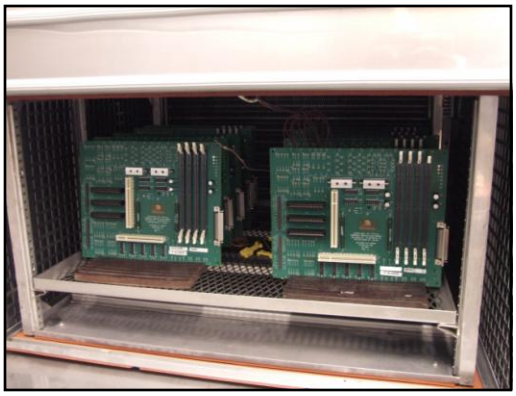

Figure 8. ATC Oven Setup

Figure 9. HTS Oven Setup

Table 8. Static and Dynamic Load Test Matrix

Board	Alloy	Thermal Shock	Mechanical		Bow & Twist	Spring		ATC (0-100°C)	HTS (125°C)
			Shock	Vibe		UA1-2	UA3-4		
7-1-001	SnPb	5 cyc (-40/+65c)	x	x	3%	16 lbs	32 lbs		x
7-1-002	SnPb	5 cyc (-40/+65c)			3%	32 lbs	16 lbs		x
7-1-003	SnPb	5 cyc (-40/+65c)	x	x		16 lbs	32 lbs	x	
7-1-004	SnPb	5 cyc (-40/+65c)				32 lbs	16 lbs	x	
7-2-001	SAC 405	5 cyc (-40/+65c)	x	x	3%	16 lbs	32 lbs		x
7-2-002	SAC 405	5 cyc (-40/+65c)			3%	32 lbs	16 lbs		x
7-2-003	SAC 405	5 cyc (-40/+65c)	x	x		16 lbs	32 lbs	x	
7-2-004	SAC 405	5 cyc (-40/+65c)				32 lbs	16 lbs	x	
7-3-001	Alloy A	5 cyc (-40/+65c)	x	x	3%	16 lbs	32 lbs		x
7-3-002	Alloy A	5 cyc (-40/+65c)			3%	32 lbs	16 lbs		x
7-3-003	Alloy A	5 cyc (-40/+65c)	x	x		16 lbs	32 lbs	x	
7-3-004	Alloy A	5 cyc (-40/+65c)				32 lbs	16 lbs	x	
7-4-001	Alloy B	5 cyc (-40/+65c)	x	x	3%	16 lbs	32 lbs		x
7-4-002	Alloy B	5 cyc (-40/+65c)			3%	32 lbs	16 lbs		x
7-4-003	Alloy B	5 cyc (-40/+65c)	x	x		16 lbs	32 lbs	x	
7-4-004	Alloy B	5 cyc (-40/+65c)				32 lbs	16 lbs	x	
7-5-001	Alloy C	5 cyc (-40/+65c)	x	x	3%	16 lbs	32 lbs		x
7-5-002	Alloy C	5 cyc (-40/+65c)			3%	32 lbs	16 lbs		x
7-5-003	Alloy C	5 cyc (-40/+65c)	x	x		16 lbs	32 lbs	x	
7-5-004	Alloy C	5 cyc (-40/+65c)				32 lbs	16 lbs	x	

Results and Discussion

Wave Profile Optimization DoE

The final wave profiles were optimized based on inspecting the overall total wave defects, including barrel fill defects and visual defects. The statistical output from the SnPb DoE is illustrated in Figure 10 below. The main effects plot indicates that there is a significant difference between the low and high level contact times used, with the lower contact time setting (i.e. higher conveyor speed) providing fewer overall defects. It also shows that the two preheat levels selected have no statistical difference between them, but indicates that the higher preheat temperature used provides slightly better results. Based on these results the optimized SnPb settings were selected and are shown in Table 9.

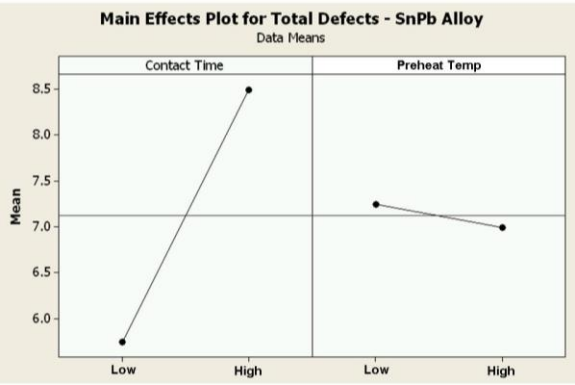

Figure 10. SnPb DoE Main Effects Plot

Table 9. SnPb Optimized Settings

Alloy	Preheat Temperature (°C)	Contact Time (secs)
SnPb	High	Low

The statistical outputs from the Pb-free optimization DoE are illustrated in Figure 11 and 12. Across all of the Pb-free alloys, the overall trend indicated that the higher pot temperature resulted in the fewest overall defects. In addition, the results for each of the alloys indicated that the higher contact time (or lower conveyor speed), although not statistically different from the lower level setting, resulted in fewer defects. Finally, the results showed that the lower preheat setting provided a statistically significant improvement in overall defects, compared to the higher preheat setting (similar to that of SnPb). Again, the levels selected for contact time and preheat temperature were based on the recommendations from the flux supplier for the specific flux used in this experiment. The final Pb-free optimized settings selected are illustrated in Table 10. The optimal settings for each Pb-free alloy were found to be identical, which can be seen based on the trend lines plotted in Figure 12. Another observation, based on the interaction plot, was related to the process window of each alloy. It can be seen that SAC405 and Alloy B exhibit a slightly larger process window within the levels of each factor selected in this DoE. It can also be seen that all of the alternative Pb-free alloys were either at least equivalent to, if not better than SAC405, in terms of total defects.

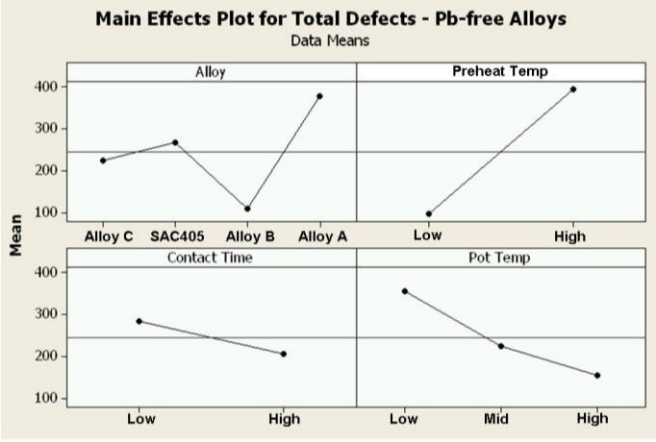

Figure 11. Pb-free DoE Main Effects Plot

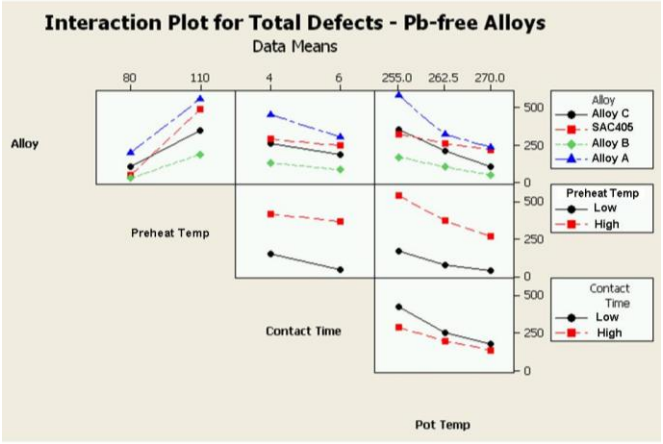

Figure 12. Pb-free DoE Interaction Plot

Table 10. Pb-free Optimized Settings

Alloy	Preheat Temperature (°C)	Contact Time (secs)	Pot Temperature (°C)
SAC405	Low	High	High
Alloy A			
Alloy B			
Alloy C			

General Process Performance (using optimized profiles)

The following results compare the total defects produced by each alloy after assembling test vehicles using the optimized wave profile (Figure 13). The results of the optimized assembly show that there is no statistical difference among SAC405 and Alloy A and B, when analyzing overall wave defects as the response. Alloy C did not perform as well, resulting in a large distribution of overall defects and a mean defect level statistically higher than SAC405, Alloy A and B. These results, along with other contributing factors, were the basis for selecting Alloy A and B, along with SAC405, (baseline) to be included in the ATC (0-100C), 6,000 cycle testing phase. In addition, all PTH and SMT fillet formations were acceptable for all alloys. There were some variations observed in solder volume, especially for Alloy C, however, they were within acceptable limits. Typical fillet formations of the capacitors assembled using Pb-free alloys are illustrated in Figure 14 a-d below as an example of the 0805 capacitor fillet formations.

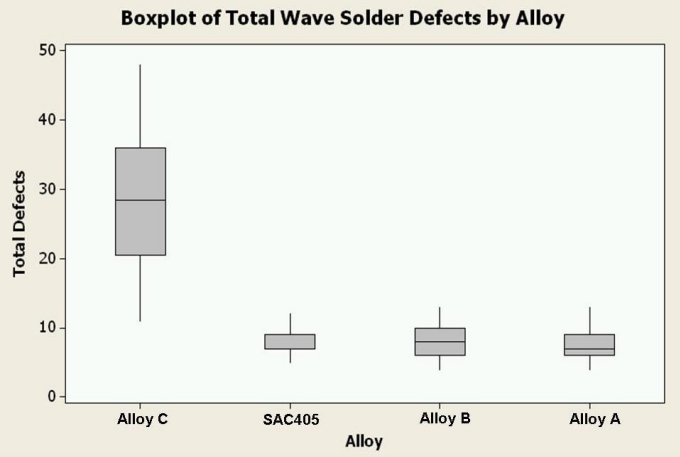

Figure 13. Boxplot of Total Wave Defects for Pb-free Alloys

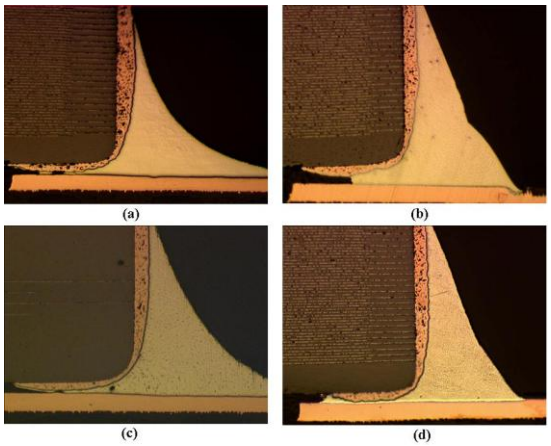

Figure 14. (a) SAC405; (b) Alloy A; (c) Alloy B; (d) Alloy C

Barrel Fill

With respect to barrel fill defects, all three alternative Pb-free alloys had relatively low levels of defects, with no statistically significant difference between them. However, all alternative alloys had a statistically higher level of barrel fill defects compared to SAC405 (Figure 15). Comparing the three alternative Pb-free alloys, Alloy C had a slightly larger distribution in barrel fill defects. Also, note that all barrel fill defects occurred on barrels which were attached to multiple ground connections. Examples of the worst case barrel fill results using Pb-free alloys are illustrated in Figure 16 a-d. As expected, all SnPb boards passed IPC, Class 2 specifications for barrel fill.

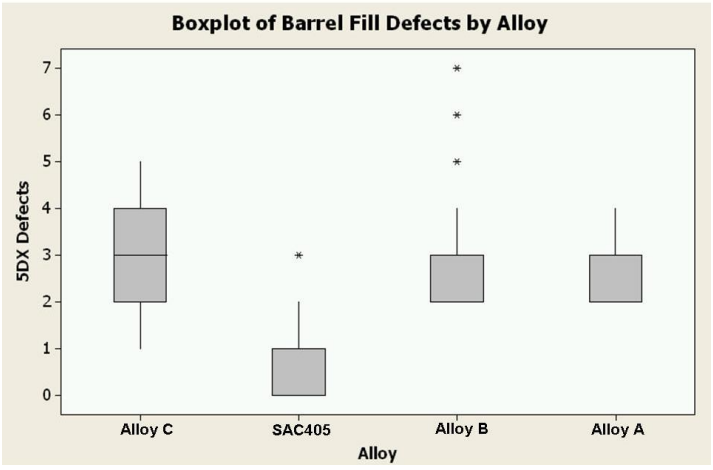

Figure 15. Boxplot of Barrel Fill Defects for Pb-free Alloys

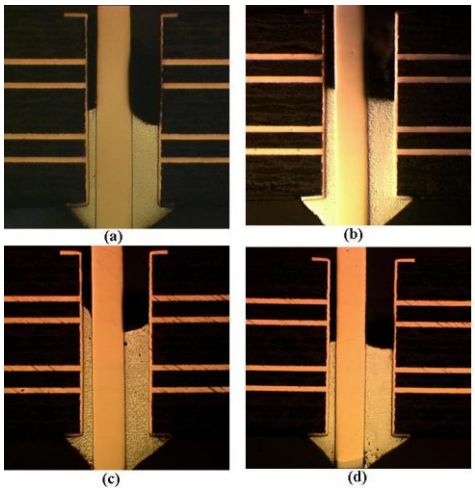

Figure 16. (a) SAC405; (b) Alloy A; (c) Alloy B; (d) Alloy C

All Pb-free alloys exhibited good wetting to the pin and barrel wall. Among all the time zero samples cross-sectioned, one sample from Pb-free Alloy B had a defect consisting of a crack through the bulk solder, propagating from the topside (Figure 17). This crack would not result initially in an open or failed joint, but could propagate to failure during ATC testing. In addition, no fillet lifting or voiding was observed in the PTH samples cross-sectioned across all alloys.

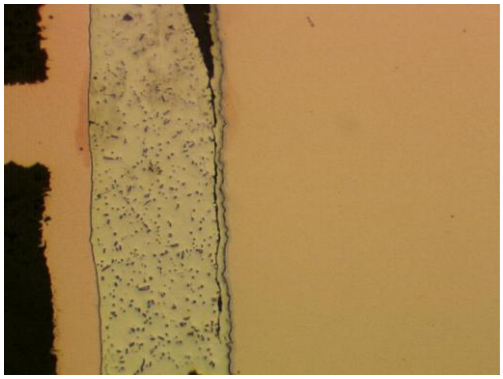

Figure 17. Time Zero X-Section, DIMM Connector, Alloy B

Bridging and Excessive Solder

The primary visual defects were either bridging or excessive solder. The results show that Alloys A and B are statistically similar to SAC405. The visual defect results for SAC405, however, had a slightly tighter distribution of defects compared to each of the alternative Pb-free alloys studied (Figure 18). Furthermore, Alloy C resulted in the highest number of total visual defects, with solder bridging accounting for the largest discrepancy (Figure 19). Note that any bridging on the 0.5mm QFP was not counted hence was not included in the overall visual defect totals. This part was assembled specifically for lead pull testing.

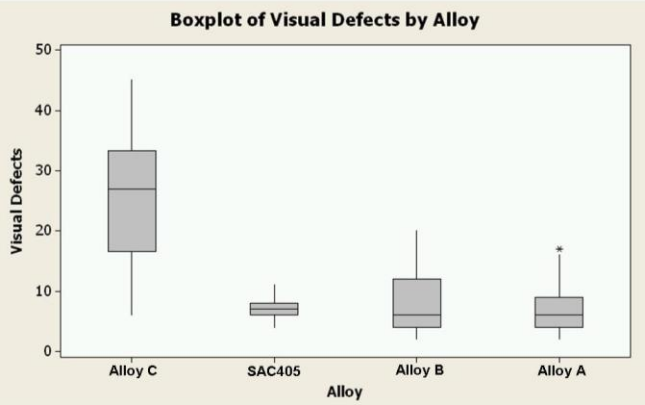

Figure 18. Boxplot of Visual Defects

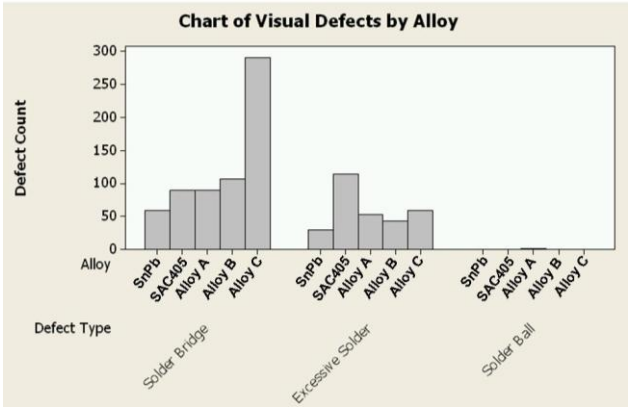

Figure 19. Chart of Visual Defects

Poor Wetting (Optimized Profile)

There were instances of poor wetting or non-wetting on the QFP, leaded device. This defect only occurred in the alternative Pb-free alloy samples (Figure 20). It was not observed when using SnPb or SAC405. These results were expected, as all of the alternative Pb-free alloys have higher melting ranges, compared to SnPb and SAC405 and each are non-eutectic alloys. These differences also explain the barrel fill results.

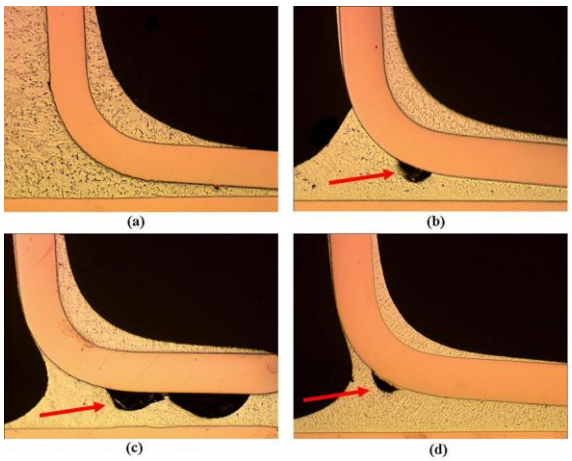

Figure 20. (a) SAC405; (b) Alloy A; (c) Alloy B; (d) Alloy C

Thermal and Mechanical Reliability Performance

4 Point Bend Test

As mentioned earlier, an array of resistors is not the standard component type evaluated with a 4 point bend test. Typically, SMT components are subjected to this test in order to validate the strength of BGA type connections. It is not usually performed to validate wave soldered connections. Even though outside the scope of the IPC specification, this test was included in an attempt to compare the mechanical strength of the alternative Pb-free alloys relative to SAC405 and SnPb in glue and wave SMT solder connections. In no case were SMT solder joint failures observed. While increases in electrical resistance were measured, it was determined through CSAM analysis that all such failures were due to cracking of the resistor bodies. Figure 21 shows an example of two cracked resistors assembled using SnPb alloy and Figure 22 shows a corresponding cross-section, illustrating the crack propagation through the component body.

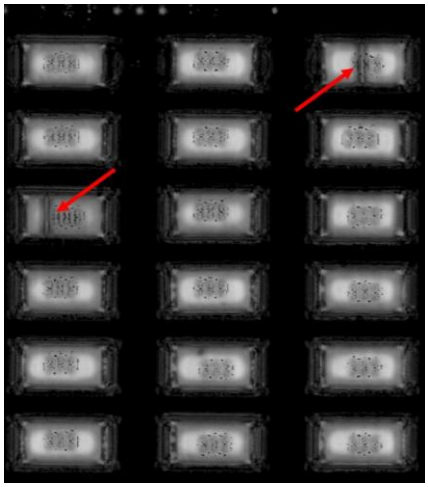

Figure 21. C-SAM, After 4-pt Bend, 6-1-005, SnPb

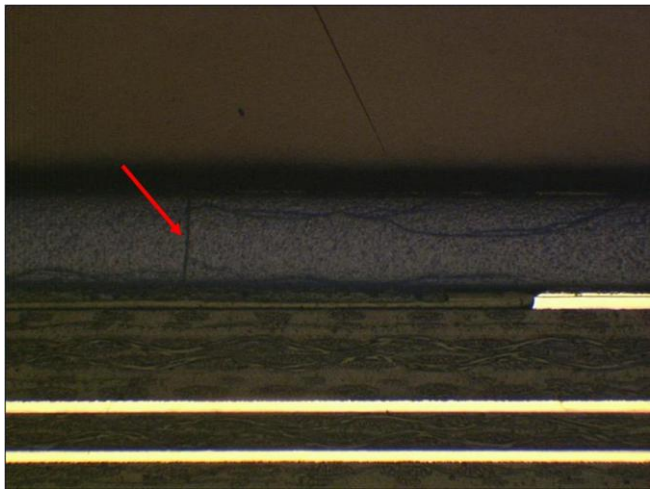

Figure 22. X-Section Crack, After 4-pt Bend, 6-1-005, SnPb

Since the failures occurred through the component bodies and not through the solder joint, a "Goodness Value" was calculated to enable a statistical analysis of the results. The "Goodness Value" was defined as the number of "passing resistors" multiplied by the deflection of the board at the time of failure. The higher the "Goodness Value", the better the result. The output based on analyzing the results using this method is illustrated in the Boxplot below (Figure 23). The results based on this analysis show that all of the Pb-free alloys are statistically similar to each other, with the SnPb alloy performing the worst overall (Figure 24). Although statistically similar, the SnPb alloy resulted in the highest amount of resistors cracking during testing. Although the mechanical test did not result in any solder joint failures, it can be theorized that greater strength of the Pb-free alloys, compared to SnPb, allowed a greater number of resistors to survive the bend test.

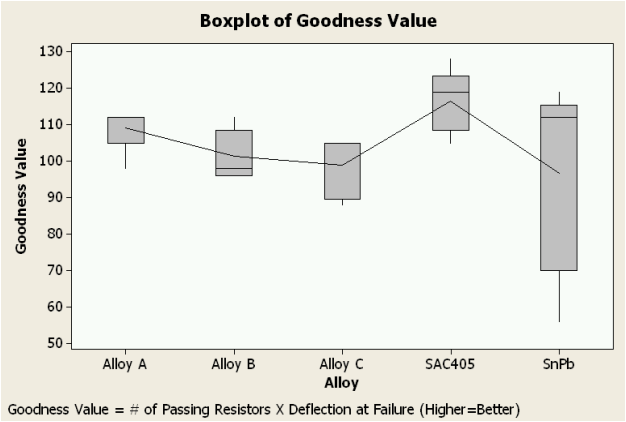

Figure 23. Boxplot of "Goodness Value"

Level	N	Mean	StDev	Individual 95% CIs For Mean Based on Pooled StDev
Alloy A	5	109.20	6.26	(----------*----------)
Alloy B	5	101.40	6.99	(----------*----------)
Alloy C	5	98.80	8.56	(----------*----------)
SAC405	5	116.60	8.62	(----------*----------)
SnPb	5	96.60	26.38	(----------*----------)

84 96 108 120

Figure 24. 4-Pt Bend Analysis of Variance (ANOVA) Output

Lead Pull Test

The statistical results of the lead pull test are illustrated in Figure 25 and 26. The Boxplot is the distribution of the maximum force (lbf) required to produce a solder-to-solder failure. Any pad-lifts which occurred during the lead pull test were not included in the results. All of the Pb-free alloys resulted in at least one pad-lift failure. There were no occurrences of pad-lift during the SnPb lead pulls. The results show a statistical difference in lead pull strength between all Pb-free alloys compared to the SnPb alloy. On average, the Pb-free alloys failed at a mean force which was 1.5X greater than that of the SnPb alloy. Alloy B performed the best overall, with results which were statistically better than Alloy A and Alloy C. Most importantly, within the grouping of Pb-free alloys, there was no statistical difference between SAC405 and any of the alternative Pb-free alloys tested.

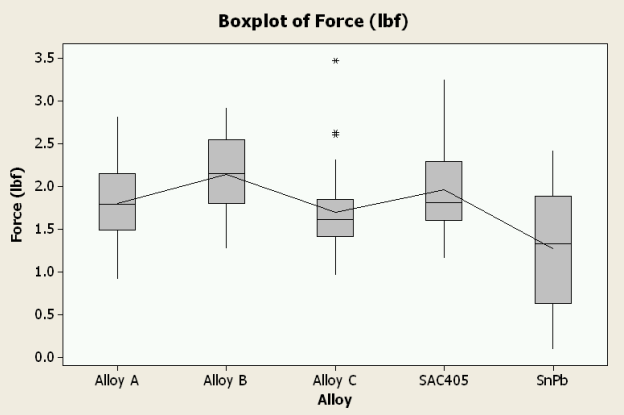

Figure 25. Boxplot of Max Force (lbf)

Level	N	Mean	StDev	Individual 95% CIs For Mean Based on Pooled StDev
Alloy A	48	1.8079	0.4528	(----*----)
Alloy B	46	2.1396	0.4361	(----*----)
Alloy C	46	1.6959	0.4339	(----*----)
SAC405	36	1.9614	0.4980	(----*-----)
SnPb	48	1.2781	0.6897	(----*---)

1.20 1.50 1.80 2.10

Figure 26. Lead Pull Analysis of Variance (ANOVA) Output

Static and Dynamic Load Testing

Static and dynamic load testing demonstrated consistently superior performance for all Pb-free alloys relative to the SnPb eutectic alloy. In fact, none of the Pb-free PTH solder joints exhibited fragility issues in the selected dynamic load environments, contrary to what has been previously reported when testing BGA type devices under similar conditions [11,12]. The ATC and HTS performance at 2000 cycles and 2000 hours readouts respectively are illustrated below (Figure 27 and Figure 28). Note that projected life estimates (in red) were made for those cells that had not failed (16 lb spring force samples) at the time of this report. These estimates were made based on extrapolation of observed plastic deformation versus expected fixed strain to failure. All U-clips exposed to a 32 lb spring load failed, under both ATC and HTS environments. At this spring force, there is no statistical difference among the grouping of alternate Pb-free alloys compared to SAC405 under ATC testing (Figure 29), however, under HTS testing a statistical difference exists (Figure 30). The superior creep resistance of SAC405 was very clearly illustrated in the 125°C isothermal HTS environment, where expected product life would be several thousand times more than SnPb under moderate load conditions. The low dissolution alloys all exhibited superior performance compared to SnPb as well, but none approached the performance of SAC405.

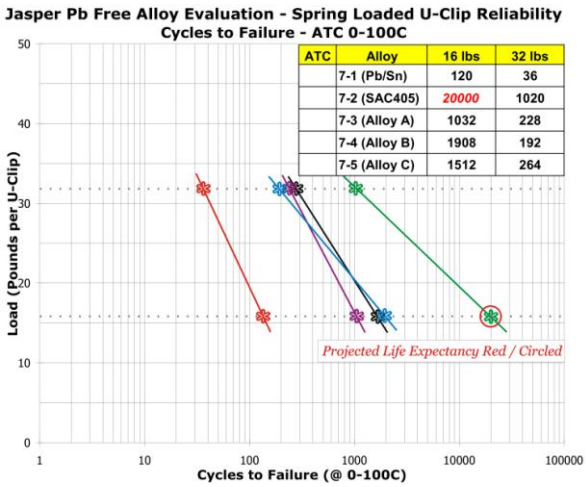

ATC	Alloy	16 lbs	32 lbs
	7-1 (Pb/Sn)	120	36
	7-2 (SAC405)	20000	1020
	7-3 (Alloy A)	1032	228
	7-4 (Alloy B)	1908	192
	7-5 (Alloy C)	1512	264

Figure 27. ATC Results, Spring Loaded U-clips

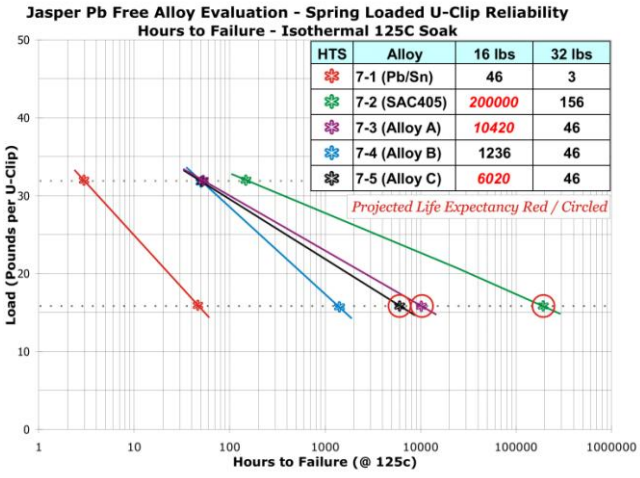

HTS	Alloy	16 lbs	32 lbs
	7-1 (Pb/Sn)	46	3
	7-2 (SAC405)	200000	156
	7-3 (Alloy A)	10420	46
	7-4 (Alloy B)	1236	46
	7-5 (Alloy C)	6020	46

Figure 28. HTS Results, Spring Loaded U-clips

Level	N	Mean	StDev	Individual 95% CIs For Mean Based on Pooled StDev
Alloy A	2	228.0	118.8	(---------*---------)
Alloy B	2	192.0	0.0	(---------*---------)
Alloy C	2	264.0	67.9	(---------*---------)
SAC405	2	1020.0	492.1	(---------*---------)
				0 500 1000 1500

Figure 29. ATC Analysis of Variance (ANOVA) Output

Level	N	Mean	StDev	Individual 95% CIs For Mean Based on Pooled StDev
Alloy A	2	46.00	0.00	(--------*-------)
Alloy B	2	46.00	0.00	(--------*-------)
Alloy C	2	46.00	0.00	(--------*-------)
SAC405	2	156.00	50.91	(-------*-------)
				0 60 120 180

Figure 30. HTS Analysis of Variance (ANOVA) Output

Each of the spring loaded U-clips under both HTS and ATC exhibited significant plastic deformation prior to failure (Figure 31). All alloys exhibited a consistent full cohesive separation of solder near the pin to solder interface on all U-clip samples (Figure 32 and 33). CT XRAY inspection was used to characterize the remaining solder joint of a severely damaged pin and is illustrated in Figure 34. The damage due to ATC was visible on all boards at the 2000 cycle inspection interval. The most obvious fatigue damage was evident at the ends of the very large DIMM and PCI connectors (Figure 35). All Pb-free alloys exhibited reduced fillet fracture damage as compared to SnPb. The 3% induced bow and twist deformation (Figure 36a) was found to generally have very little effect on most of the devices on these boards for all alloys, including SnPb. Even the very large DIMM and PCI connectors which exhibited the most obvious damage in the ATC cells had no damage in the HTS bow and twist cells. Surprisingly, the small 14-pin PDIP locations U102 and U104 were the only sites which exhibited damage due to the bow and twist (Figure 36b). The SnPb alloy exhibited severe gaping fractures at both of these locations, while the low dissolution Pb-free alloys all had no visible damage. The connectors assembled with SAC405 alloy showed a small fillet fracture at U102 location (Figure 37).

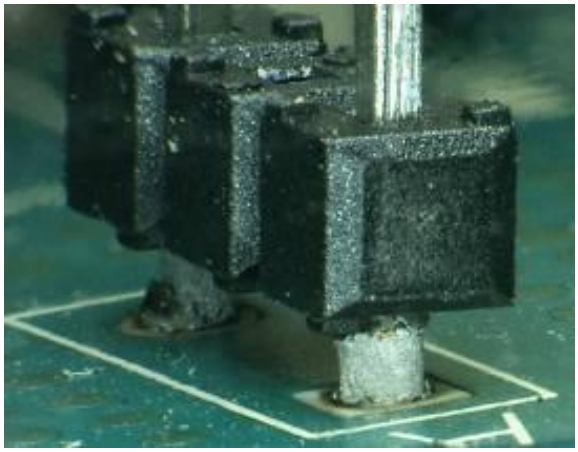

Figure 31. HTS/ATC damage, Spring Loaded U-clips

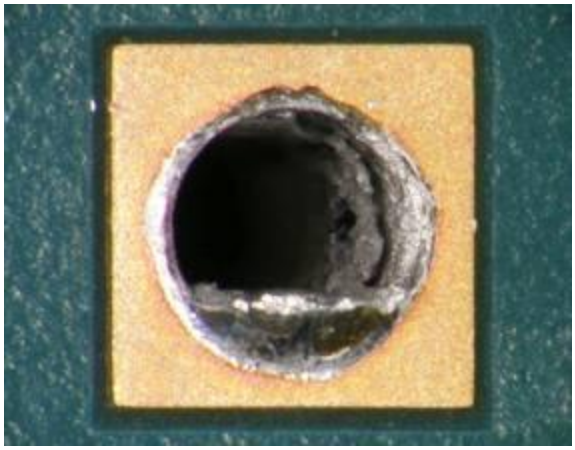

Figure 32. Raw card after failure of U-clips

Figure 33. Typical appearance of fractured U-clip pins

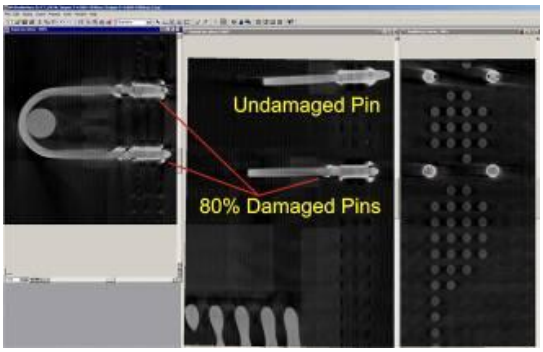

Figure 34. CT XRAY Image of Spring Loaded U-clips

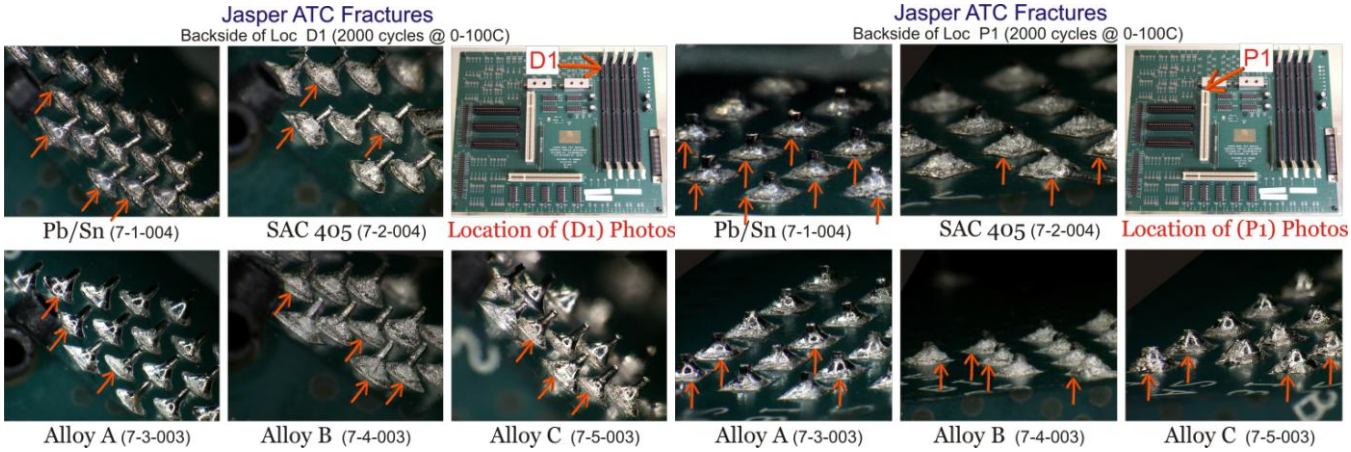

Figure 35. ATC Results, Solder Joint Fatigue at D1, P1 Locations

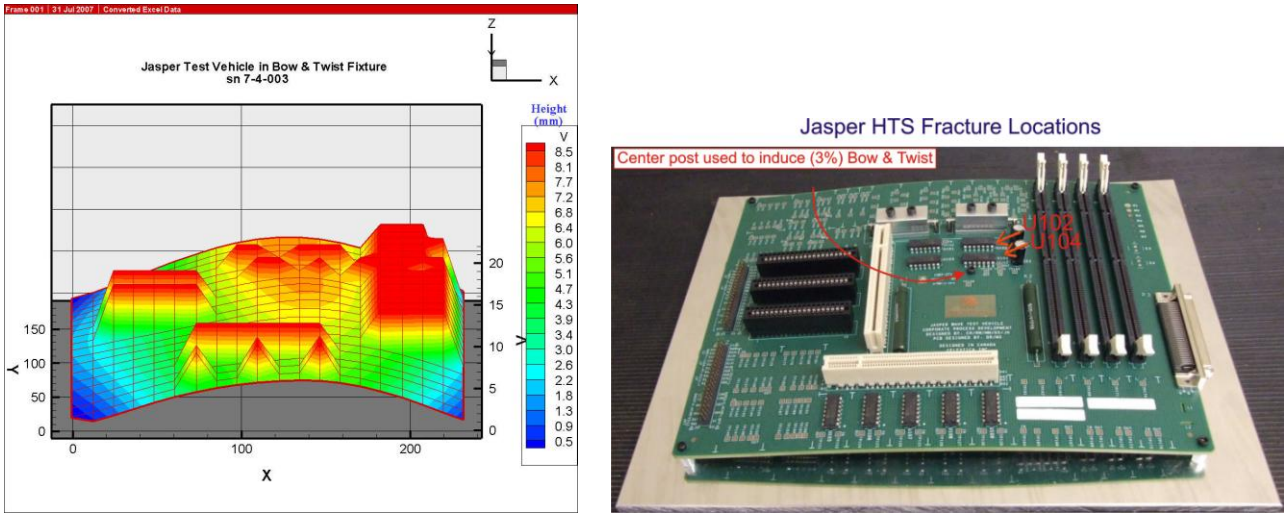

(a) **(b)**

Figure 36. (a) Card shape measurements, 3% Bow and Twist Fixture;
(b) Location of HTS fracture damage (U102, U104) induced by 3% Bow and Twist Fixture

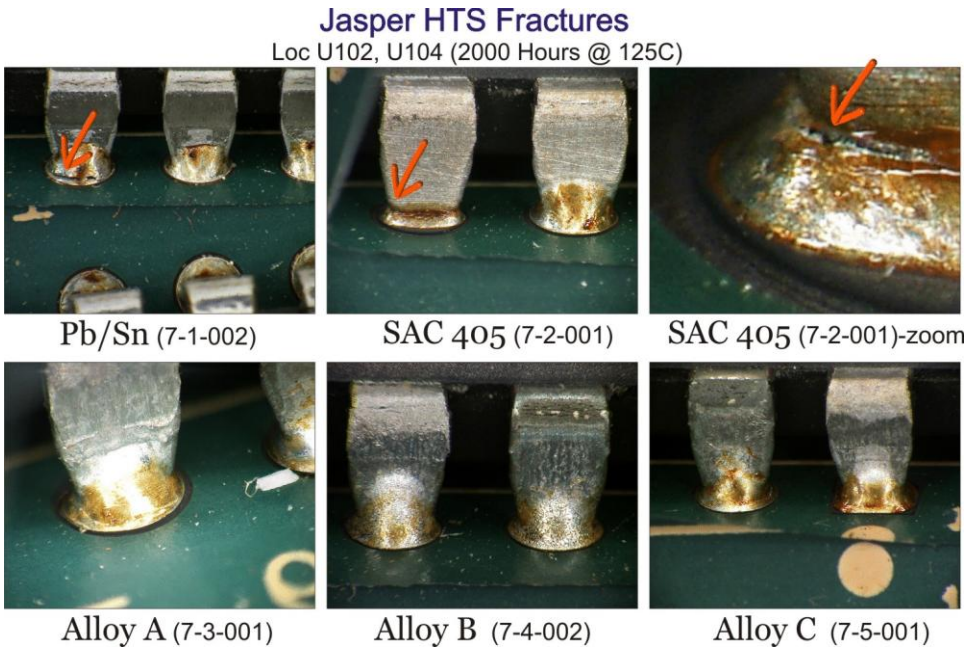

Figure 37. HTS Results, Photos of U102, U104 Locations with fractures induced by 3% Bow and Twist Fixture

Summary

In summary, the process performance results indicated that two out of the three alternative Pb-free alloys tested (Alloy A and B) were comparable to SAC405 with respect to overall wave solder assembly yields. However, all of the alternative Pb-free alloys resulted in statistically higher levels of barrel fill defects, compared to the SAC405 baseline. In one case, a crack propagating from the topside was observed in a PTH joint, assembled using Alloy B. This crack was not an issue at time zero, but could propagate during ATC or mechanical + thermal type testing, potentially resulting in an open (or failed) connection. With respect to the total visual defects (i.e. bridging, excessive solder), Alloys A and B were statistically similar to SAC405 in total quantity. Alloy C, however, produced a significantly higher degree of visual defects. In addition, non-wetting between the solder and a leaded device was observed in samples assembled using each of the three alternative Pb-free alloys. There was no occurrence of non-wetting on the SAC405 or SnPb samples cross-sectioned. Although the sample size for this experiment was relatively small to predict yield comparisons for manufacturing volumes, the results do provide a good ranking for the general performances of each alternative Pb-free alloy compared to SAC405.

The results of the two mechanical tests (i.e. 4 point bend and lead pull), provided two main outcomes: 1) Each of the alternative Pb-free alloys included in this study is equivalent if not better than SAC405 and 2) Each of the alternative Pb-free alloys, in addition to SAC405, is far superior to the performance of SnPb. This result indicates that the strength of the joints formed by the alternative alloys is equivalent to that of SAC405, hence capable of surviving as long as SAC405 when exposed to similar forces. The static and dynamic load testing, under thermal and mechanical conditions, also showed that each of the Pb-free alloys tested significantly outlasted the SnPb alloy. However, in this case, the SAC405 alloy was far superior to that of the three alternative Pb-free alloys, in part due to the superior creep resistance of SAC405. That being said, all Pb-free alloys tested would be expected to deliver superior performance to SnPb on boards with static loads induced from assembly, mounting conditions, or high mechanical load requirements of the product.

Conclusion

The main objective of this study is to identify potential alternative Pb-free wave alloys and validate their capability of replacing SAC305/405 alloys in both the PTH rework and wave soldering processes. The results from this study, based on the process performance, mechanical testing and preliminary results of the thermal/mechanical testing indicate that at least two out of the three alternative Pb-free alloys tested are potential suitable replacements to SAC305/405 at the wave solder and solder fountain processes. However, the results of the thermal reliability ATC testing and forced rework evaluations are still required before drawing final conclusions. Based on the results, along with other contributing factors, Alloy A and B, along with SAC405 (baseline) were selected to be included in the ATC (0-100°C), 6,000 cycle testing phase. The table below (Table 11) summarizes the results of each test, in ranking order by alloy. Those cells highlighted in yellow indicate that the alloy results were statistically similar to that of SAC405.

Table 11. Final Alloy Ranking Results by Test Phase

ALLOY	Process Performance				Mechanical Reliability		*Mechanical + Thermal Reliability		Thermal Reliability
	Primary Attach		*Rework*		*Primary Attach*		*Primary Attach*		Primary/Rework
	Barrel Fill	Visual	Process	Defects	4-pt Bend	Lead Pull	ATC, 0-100°C	HTS (@ 125°C)	ATC, 0-100°C
SnPb	1st	1st	TBD	TBD	5th	5th	5th	5th	Not testing
SAC405	2nd	2nd	TBD	TBD	1st	2nd	1st	1st	TBD
Alloy A	3rd	3rd	TBD	TBD	2nd	3rd	3rd	2nd	TBD
Alloy B	3rd	4th	TBD	TBD	3rd	1st	4th	2nd	TBD
Alloy C	4th	5th	TBD	TBD	4th	4th	2nd	2nd	Not testing

Statistically similar to SAC405, based on a 95% confidence interval

* Partial testing results at 2,000 cycles/hours, using 32lb sping load results

The test results to date indicate that the implementation of an alternative Pb-free alloy to mitigate the occurrence of Cu dissolution during PTH rework and establish a common alloy for the PTH assembly and rework processes may result in an increased difficulty of achieving barrel fill. The results, however, indicate that the barrel fill performance of some of the alternative Pb-free alloys tested was within a reasonable range of overall defects. Further optimization of the wave profile and/or further flux optimization may contribute to improved barrel fill of the alternative alloys, bringing it on par with SAC405. In addition, further studies of board design (i.e. pin-to-hole ratio, ground connection layer counts and style) contributions could be required to achieve appropriate levels of barrel fill (using any Pb-free alloy selected). Design optimization may be especially important when soldering to boards which are thermally massive (>200 mil thick, with multiple ground layers) and/or are required to meet current IPC-A-610D, Class 3 specifications (i.e. ≥75% barrel fill for all PTH connections).

Future Work

Future work includes additional reliability testing and a rework evaluation. The ATC, 0-100°C reliability testing is scheduled to conclude after 6,000 cycles. This reliability test is commonly required to satisfy some consumer, data processing and telecommunication product requirements. In addition, data is also required on the impact of harsh environments (i.e. -55 to 125°C) on the thermal fatigue reliability of these alternative Pb-free wave alloys. This harsh environment testing is a key requirement for Aerospace and Defense OEMs. The rework evaluation will compare process factors such as overall cycle time for the various alloys and reliability trends such as the survival of reworked vs. primary attach connections during ATC and the impact of rework on the mechanical integrity of reworked connectors. In addition, future work will include studying the impact of various Cu dissolution levels on the thermal fatigue reliability of a PTH joint.

Acknowledgements

The authors would like to extend our appreciation to each of the participating solder suppliers as well as acknowledge the organizational support of both IBM and Celestica that enabled this study. The consultations provided by Jim Wilcox and Marie Cole of IBM and Linda Scala, Thilo Sack and Irene Sterian of Celestica were particularly helpful. Special thanks are also due the Celestica design team, Denesh Ramsamujh and Malcolm Simpson, and the respective laboratory support teams from Celestica (Zohreh Bagheri, Jason Bragg, Bob Buick, Jie Qian, Subramaniam Suthakaran and Michael Thomson) and IBM (Dave Braun, John Kan, and Miles Swain). Metallurgical analyses were provided by Polina Snugovsky of Celestica.

References

[1] D. Barbini, P. Wang, et. al., "Lead Free Wave Soldering: Influence of Alloys, Board Design, and Process Parameters on Defect Formation", Proceeding of SMTAi International, October 2007.

[2] C. Hamilton, P. Snugovsky, PhD, Celestica, M. Kelly, IBM "A Study of Copper Dissolution during Pb-free PTH Rework using a Thermally Massive Test Vehicle", Proceedings of SMTAi International, September 2006.

[3] F. Boyle, D. Jean, Plexus, D. Lee, Boston Scientific "A Study of Copper Dissolution in Pb-Free Solder Fountain Systems", Proceedings of SMTA International, September 2006.

[4] C. Hamilton, P. Snugovsky, PhD, Celestica, M. Kelly, IBM "Have High Cu Dissolution Rates of SAC305/405 Alloys Forced a Change in the Lead Free Alloy used during PTH Processes?", Proceedings of Pan Pacific Microelectronics, January 2007.

[5] J. Gleason, C. Reynolds, "iNEMI Advanced Lead Free Assembly and Rework Project", April 2005.

[6] D. Hillman, et. al., "JCAA/JGPP Lead Free Solder Project", Proceeding of SMTAi International, 2005.

[7] H. Holder, et. al., "Reliability of Partially Filled SAC305 Through Hole Joints", Proceedings of APEX, 2006.

[8] J. Nguyen, et. al., "Process and Reliability Study of Lead Free Wave Soldering for Large Thick Boards", Proceeding of SMTAi International, October 2007.

[9] IPC, "IPC-A-610D Acceptability of Electronic Assemblies" February 2005.

[10] IPC, "IPC/JEDEC-9702 Monotonic Bend Characterization of Board-Level Interconnects" June 2004.

[11] P. Lall, et. al., Auburn University Dept of Mechanical Engineering and NSF Center for Advanced Vehicle Electronics, "Models for Shock and Vibration Survivability of Electronic and MEMS Packaging", Proceedings of ASME InterPACK, July 2005.

[12] D. Chong, et. al., Drop Impact Reliability Testing for Lead-Free and Lead-Based Soldering IC Packages", Proceedings of Elsevier, Microelectronics Reliability, September 2005.